Spatial $\mathcal{H}_2$ Control of a Piezoelectric Laminate Beam: Experimental Implementation

Dunant Halim, *Student Member, IEEE,* and S. O. Reza Moheimani, *Senior Member, IEEE*

***Abstract*—The aim of this paper is to design and experimentally evaluate the performance of a feedback controller to suppress vibration of a flexible beam. The controller is designed to minimize the spatial $\mathcal{H}_2$ norm of the closed-loop system to ensure average reduction of vibration throughout the entire structure. Vibrations of the first six bending modes of the beam are to be controlled using a collocated piezoelectric actuator-sensor pair attached to the beam. Feedthrough terms are incorporated into the flexible-structure model to correct the locations of the in-bandwidth zeros. It is shown that the spatial $\mathcal{H}_2$ control has an advantage over the pointwise $\mathcal{H}_2$ control in minimizing the vibration of the entire structure. The spatial $\mathcal{H}_2$ controller minimizes the $\mathcal{H}_2$ norm of the entire structure more uniformly, while the pointwise $\mathcal{H}_2$ controller only has a local effect. The implemented spatial $\mathcal{H}_2$ controller is able to minimize the first six bending modes of the beam effectively. This spatial $\mathcal{H}_2$ control can also be applied to more general structural vibration suppression problems.**

***Index Terms*—$\mathcal{H}_2$ control, flexible structures, intelligent structures, piezoelectric transducers, spatial $\mathcal{H}_2$ norm, vibration control.**

I. Introduction

MANY engineering applications use structures that can be considered to be flexible. Flexible structures are distributed parameter systems. Therefore, vibration of each point is dynamically related to the vibrations of every other point over the structure. It is important to design a controller with a view to minimizing structural vibrations of the entire structure, rather than a limited number of points. This would ensure that structural vibrations of the entire structure is suppressed.

This paper presents experimental implementation of the concept of spatial $\mathcal{H}_2$ control on a piezoelectric laminate beam for the first time. The controller is designed such that the spatial $\mathcal{H}_2$ norm of the closed-loop system is minimized. Minimizing the spatial $\mathcal{H}_2$ norm of the system will ensure vibration suppression over the entire structure in an average sense. The spatial $\mathcal{H}_2$ control problem can be solved by finding an equivalent system representation that allows a standard $\mathcal{H}_2$ control optimization problem to be solved instead.

The spatial $\mathcal{H}_2$ control produces a controller with similar dimensions as that of the plant. If a model is developed via the modal analysis technique, a direct truncation can be used to obtain a finite-dimensional model of the system. However, it is known that the locations of the in-bandwidth zeros are not accurate because of the truncation of high-frequency dynamics [1]–[4]. This inaccuracy can have negative effect on the closed-loop stability. To fix this problem, feedthrough terms are added to the model to correct the locations of the zeros as discussed in [1]–[4]. This technique is known in the aeroelasticity literature as the mode acceleration method [5].

To demonstrate the proposed controller, a single-input–single-output (SISO) spatial $\mathcal{H}_2$ controller is designed for a piezoelectric laminate beam to suppress the vibration of the first six bending modes of the structure. The controller is implemented on the structure, a simply-supported beam with a collocated piezoelectric actuator-sensor pair.

Piezoelectric actuators and sensors have been used in many vibration control applications of flexible structures [6]–[12]. Piezoelectricity was discovered in 1880 by French scientists Pierre and Paul-Jacques Curie. The piezoelectric effect is observed in many crystalline materials, which strain when exposed to a voltage and produce a voltage when strained. In other words, these materials are capable of transforming mechanical energy into electrical energy and *vice versa*. In the experiments, piezoelectric actuators and sensors are used.

This paper is organized as follows. Section II describes the dynamics of flexible structures with collocated piezoelectric actuator-sensor pairs. Section III describes the notion of spatial $\mathcal{H}_2$ norm that is used as a performance measure for flexible structures. Section IV deals with the model correction to reduce the error in the locations of the in-bandwidth zeros of the model. Section V describes the concept of spatial $\mathcal{H}_2$ control for flexible structures. Section VI discusses the design of a feedback SISO controller for suppressing the vibration of the first six bending modes of a simply supported piezoelectric laminate beam. Section VII presents experimental implementation of the controller on a beam structure. The last section draws conclusions. The modal solution of a simply supported beam is included in Appendix.

II. Models of Flexible Structures

This section briefly explains how a model of a beam with a number of collocated piezoelectric actuator-sensor pairs can be obtained using a modal analysis technique. Interested readers can refer to [8], [9] for more detailed derivations.

Consider a homogeneous Euler–Bernoulli beam with length L, width W and thickness h as shown in Fig. 1. The piezoelectric actuators and sensors have length L_{px}, width L_{py} and thickness h_p. In this paper, $h_p \ll h$ is assumed, which is true for the patches that are used in experiments. Thus, the assumption of

Manuscript received November 27, 2000. Manuscript received in final form February 27, 2002. Recommended by Associate Editor E. G. Collins, Jr.

The authors are with the School of Electrical Engineering and Computer Science, University of Newcastle, NSW, Australia (e-mail: dunanth@ee.newcastle.edu.au; reza@ee.newcastle.edu.au).

Publisher Item Identifier S 1063-6536(02)05355-1.

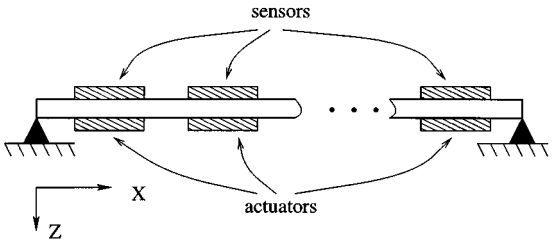

Fig. 1. A simply supported beam with a number of collocated piezoelectric patches.

uniform beam properties can be justified. However, approximation methods such as the finite element method can also be used to deal with more general nonuniform structures.

Suppose there are M collocated actuator-sensor pairs distributed over the structure. Piezoelectric patches on one side of the beam are used as sensors, while patches on the other side are used as actuators. Voltages that are applied to actuating patches are represented by $V_a(t) = [V_{a1}(t), \ldots, V_{aM}(t)]^T$.

A model of the structure can be obtained via the modal analysis procedure. This procedure requires finding a solution to the partial differential equation (PDE) which describes the dynamics of the structure. The governing PDE of a flexible beam is as follows [7], [13]:

$$EI\frac{\partial^4 z(x,t)}{\partial x^4} + \rho A_b \frac{\partial^2 z(x,t)}{\partial t^2} = \frac{\partial^2 M_{px}(x,t)}{\partial x^2} \tag{1}$$

where the beam transverse deflection at point x and at time t is denoted by $z(x,t)$. The deflection $z(x,t)$ is assumed to be in the form of $z(x,t) = \sum_{k=1}^{\infty} W_k(x) q_k(t)$, where $W_k(x)$ is the eigenfunction and $q_k(t)$ is the time-dependent solution. Also, ρ, A_b, E, and I represent the density, the cross-sectional area of the beam, the Young's Modulus and the moment of inertia about the beam's neutral axis, respectively. The forcing moment acting on the beam is denoted by M_{px}.

The forcing moment on the beam, M_{px}, is generated by piezoelectric actuators. A voltage, V_{ai}, which is applied to the ith actuator, would produce a forcing moment, M_{px}^i

$$M_{px}^i = \bar{K}\left[H\left(x - x_{1i}\right) - H\left(x - x_{2i}\right)\right] V_{ai}(t) \tag{2}$$

where $H(\cdot)$ is a step function and x_{1i}, x_{2i} denote the ith actuator's locations along the X axis. $\bar{K}$ depends on the properties of the structure and the piezoelectric patches. Thus, the forcing moment depends on the actuator's location along the beam as well as the applied voltage.

The PDE can be solved independently for each mode by using the orthogonality properties of its eigenfunctions W_k which are as follows for the case of a uniform beam:

$$\int_0^L W_k(x) W_p(x) dx = \delta_{kp} \tag{3}$$

$$\int_0^L \frac{EI}{\rho A_b} \frac{d^4 W_k}{dx^4} W_p dx = \omega_k^2 \delta_{kp} \tag{4}$$

where ω_k describes the natural frequency of the beam at mode k. Here, δ_{kp} is Kronecker's delta function, that is, $\delta_{kp} = 0$ for all $k \neq p$ and equals one if $k = p$.

The multiple-input–infinite-output (MIIO) transfer function from the applied actuator-voltages $V_a(s)$ to the transverse structural deflection $z(s,x)$ at location x is

$$G(s,x) = \sum_{k=1}^{\infty} \frac{W_k(x) \bar{\Psi}_k^T}{s^2 + 2\zeta_k \omega_k s + \omega_k^2} \tag{5}$$

where $\bar{\Psi}_k = [\Psi_{k1}, \ldots, \Psi_{kM}]^T$ and the mode number is denoted by k. Ψ_{ki} is a function of the location of the ith piezoelectric actuator, the eigenfunction $W_k(x)$ and the properties of the structure and the piezoceramic patch (see [11], [14], and [15]). The damping ratio is denoted by ζ_k.

Such models have the interesting property that they describe spatial and spectral properties of the system. The spatial information of these models can then be used to design controllers, which guarantee a certain level of damping for the entire structure.

Furthermore, the multiple-input–multiple-output (MIMO) transfer function of the flexible structure with piezoelectric actuator-sensor (collocated) pairs can be determined in a similar manner. The transfer function from the applied actuator-voltages $V_a(s)$ to the induced voltages at the sensor $V_s(s) = [V_{s1}(s), \ldots, V_{sM}(s)]^T$ is

$$G_{Vs}(s) = \Upsilon \sum_{k=1}^{\infty} \frac{\bar{\Psi}_k \bar{\Psi}_k^T}{s^2 + 2\zeta_k \omega_k s + \omega_k^2} \tag{6}$$

where $\Upsilon > 0$ is a constant based on the properties of the structure and the piezoceramic patches.

III. Spatial $\mathcal{H}_2$ Norm

This section presents an overview of the concept of spatial $\mathcal{H}_2$ norm. Consider the transfer function of a flexible structure, $G(s,x)$, as in (5). This model describes the spatial and spectral behavior of the structure. The $\mathcal{H}_2$ norm of $G(s,x)$ can be used as a measure of performance at a particular point x. However, it cannot be used as a global performance measure for the entire structure as it is calculated based on the response at a specific location on the structure [6], [16]. To obtain a global performance measure for the entire structure, the notion of spatial $\mathcal{H}_2$ norm can be used.

The spatial $\mathcal{H}_2$ norm of the transfer function $G(s,x)$ is defined [6], [16] as,

$$\ll G \gg_2^2 = \frac{1}{2\pi} \int_{-\infty}^{\infty} \int_X tr\left\{G(j\omega,x)^* G(j\omega,x)\right\} dx d\omega \tag{7}$$

where X is the set over which x is defined. For a beam, $X = [0, L]$. Here, $tr\{\psi\}$ represents the trace of the matrix ψ. Taking advantage of the orthonormality of the eigenfunctions, W_k, in (3), it can be shown that

$$\ll G \gg_2^2 = \sum_{k=1}^{\infty} \left\| \tilde{G}_k \right\|_2^2 \tag{8}$$

where

$$\tilde{G}_k(s) = \frac{\bar{\Psi}_k^T}{s^2 + 2\zeta_k \omega_k + \omega_k^2}. \tag{9}$$

From definition (7), it can be argued that the spatial $\mathcal{H}_2$ norm is a suitable measure of performance for spatially distributed linear time-invariant systems, such as those described in (5). Furthermore, if the system can be broken into a number of orthonormal modes, then the contribution of each mode to the total spatial $\mathcal{H}_2$ norm of the system can be determined from (8) and (9). Also, since the spatial $\mathcal{H}_2$ norm of a system of the form (5) is equivalent to the $\mathcal{H}_2$ norm of a finite-dimensional system, it can be calculated using standard software.

Another way of calculating the spatial $\mathcal{H}_2$ norm of a system is to first obtain a state-space representation of the system and then to apply definition (7) to determine a finite-dimensional system whose $\mathcal{H}_2$ norm is equivalent to the spatial $\mathcal{H}_2$ norm of the spatially distributed system. To demonstrate this, suppose a state-space representation of the transfer function $G(s,x)$ can be described as

$$\begin{aligned}\dot{\bar{x}}(t) =& A\bar{x}(t) + Bw(t)\\ z(x,t) =& C(x)\bar{x}(t)\end{aligned} \tag{10}$$

where $w(t)$ are external disturbances through the actuators. Notice that for a vibratory system such as a beam, $z(x,t)$ represents the deflection at a particular point, x, along the structure. Such a model can be obtained by truncating the series (5) and keeping the first N modes. Then the spatial $\mathcal{H}_2$ norm of the transfer function $G(s,x)$ can be shown to be equivalent to [6], [16]

$$\ll G \gg_2^2 = \|\hat{G}\|_2^2 \tag{11}$$

where

$$\hat{G}(s) = \Gamma(sI - A)^{-1}B \tag{12}$$

and

$$\Gamma^T\Gamma = \int_X C(x)^T C(x)dx. \tag{13}$$

Hence, the spatial $\mathcal{H}_2$ norm of $G(s,x)$ can be determined by calculating the $\mathcal{H}_2$ norm of $\hat{G}(s)$.

In certain problems, it may be necessary to weight the output of $G(s,x)$ in a nonuniform manner. Imagine a situation where vibration of a particular region on the surface of a flexible structure is to be damped more heavily. In such a case, the definition (7) can be modified to allow for a spatially distributed weighting function. Hence, the weighted spatial 2-norm of G is defined to be

$$\ll G \gg_{2,Q}^2 = \frac{1}{2\pi}\int_{-\infty}^{\infty}\int_X tr\left\{G(j\omega,x)^* Q(x) G(j\omega,x)\right\} dx d\omega. \tag{14}$$

Note that if $Q(x)$ is chosen to be a Dirac Delta function, i.e., $\delta(x - x_1)$, (14) reduces to

$$\ll G \gg_{2,\delta}^2 = \frac{1}{2\pi}\int_{-\infty}^{\infty} tr\left\{\tilde{G}(j\omega)^*\tilde{G}(j\omega)\right\} d\omega \tag{15}$$

where $\tilde{G}(j\omega) = G(j\omega, x_1)$. Hence, definition (14) collapses to the $\mathcal{H}_2$ norm of a finite-dimensional system.

IV. Model Correction

In practice, dynamical models of a flexible structure as described in (5) and (6) have to be truncated to represent the system by a finite-dimensional model. The model can be truncated so to include only the modes within the frequency bandwidth of interest. However, the truncation of the model produces additional error in the locations of the in-bandwidth zeros. This is due to the fact that the contribution of the out-of-bandwidth modes, i.e., high-frequency modes, is generally ignored in the truncation.

One way to improve the truncated model dynamics is to include feedthrough terms to correct the locations of the in-bandwidth zeros. This technique is known in the aeroelasticity literature as the mode acceleration method [5] and has been recently revisited in [1]–[4].

Thus, the infinite-dimensional model of the collocated system in (6) can be approximated as $G_{Vs}^N(s)$

$$G_{Vs}^N(s) = \Upsilon\sum_{k=1}^{N}\frac{\bar{\Psi}_k\bar{\Psi}_k^T}{s^2 + 2\zeta_k\omega_k s + \omega_k^2} + K_{Vs} \tag{16}$$

where N is the number of modes included in the model and K_{Vs} is a $M \times M$ matrix added to correct the locations of in-bandwidth zeros. For a SISO system, K_{Vs} will be a scalar. For a general multivariable system, K_{Vs} can be found using the method proposed in [3] and [17]. This is done by determining a feedthrough term that minimizes the $\mathcal{H}_2$ norm of the difference between the infinite-dimensional and the truncated models, J_o

$$J_o = \left\|W_{co}(s)\left(G_{Vs}(s) - G_{Vs}^N(s)\right)\right\|_2^2 \tag{17}$$

$$K_{Vs} = \frac{\Upsilon}{2\omega_{co}}\sum_{k=N+1}^{\infty}\frac{\bar{\Psi}_k\bar{\Psi}_k^T}{\omega_k}\ln\left(\frac{\omega_k + \omega_{co}}{\omega_k - \omega_{co}}\right). \tag{18}$$

Here, ω_{co} is the cutoff frequency of the ideal low-pass filter, $W_{co}(s)$, which is chosen to lie within the interval (ω_N, ω_{N+1}).

Similarly, the approximate spatial transfer function of $G(s,x)$ in (5) can be described by

$$G^N(s,x) = \sum_{k=1}^{N}\frac{W_k(x)\bar{\Psi}_k^T}{s^2 + 2\zeta_k\omega_k s + \omega_k^2} + K(x) \tag{19}$$

where $K(x)$ is a $1 \times M$ vector. $K(x)$ is a function of the spatial variable, x, which has to be estimated from the modal model of the system.

One possibility is to find a feedthrough term that minimizes the weighted spatial $\mathcal{H}_2$ norm of the error between the infinite-dimensional and the truncated models [2]. The term $K(x)$ is determined such that the following cost function is minimized:

$$J_1 = \ll W_{c1}(s,x)\left(G(s,x) - G^N(s,x)\right) \gg_2^2. \tag{20}$$

Here, $W_{c1}(s,x)$ is an ideal low-pass weighting function distributed spatially over X with its cutoff frequency, ω_{c1}, chosen to lie within the interval (ω_N, ω_{N+1}).

The cost function (20) is minimized by setting [2]

$$K(x) = \sum_{k=N+1}^{\infty} K_k^{opt} W_k(x) \tag{21}$$

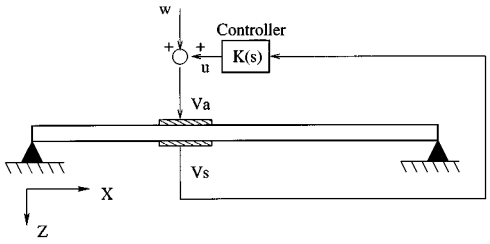

Fig. 2. Spatial $\mathcal{H}_2$ control of a flexible beam.

Fig. 3. Experimental apparatus.

where

$$K_k^{opt} = \frac{1}{2\omega_{c1}\omega_k} \ln\left(\frac{\omega_k + \omega_{c1}}{\omega_k - \omega_{c1}}\right) \bar{\Psi}_k^T. \tag{22}$$

Note that in practice only a finite number of modes can be included in order to calculate the feedthrough term, $K(x)$. This should not cause a major problem as the effect of modes will diminish with increasing k.

V. Spatial $\mathcal{H}_2$ Control of a Piezoelectric Laminate Beam

This section is concerned with the problem of spatial $\mathcal{H}_2$ control for flexible structures. Consider a typical system of a flexible structure such as the one shown in Fig. 2. The system consists of only one piezoelectric actuator-sensor pair for the sake of clarity. Here, the purpose of the controller is to reduce the effect of disturbance, $w(t)$, on the entire structure, using piezoelectric actuators and sensors. The concept of spatial $\mathcal{H}_2$ control was introduced in [6], [16] to address problems of this nature.

A spatially distributed linear time-invariant dynamical system such as the beam in Fig. 2 can be defined in its state-space form as

$$\begin{aligned} \dot{\bar{x}}(t) &= A\bar{x}(t) + B_1 w(t) + B_2 u(t) \\ z(x,t) &= C_1(x)\bar{x}(t) + D_{11}(x)w(t) + D_{12}(x)u(t) \\ V_s(t) &= C_2\bar{x}(t) + D_{21}w(t) + D_{22}u(t) \end{aligned} \tag{23}$$

where $\bar{x} \in \mathbf{R}^n$ is the state, $w \in \mathbf{R}$ is the disturbance input, $u \in \mathbf{R}$ is the control input, z is the performance output, $V_s \in \mathbf{R}$ is the measured output. For a flexible structure, $z(x,t)$ represents the spatial displacement at time t, where $x \in X$.

The system matrices in (23) can be obtained from transfer functions (16) and (19). Note that for the system shown in Fig. 2, $D_{22} = D_{21}$ in (23) is the feedthrough term K_{Vs} described in (16), while $D_{11}(x) = D_{12}(x)$ is $K(x)$ in (21). Moreover, $B_1 = B_2$ since disturbance is assumed to enter the system through the actuator.

TABLE I
Properties of the Piezoelectric Laminate Beam

Beam X-length, L	0.600 m
Beam width, W	0.050 m
Beam thickness, h	0.003 m
Beam Young's Modulus, E	7.00×10^{10} N/m^2
Beam density, ρ	2.770×10^3 kg/m^3
Piezoceramic X-length, L_{px}	0.070 m
Piezoceramic Y-length, L_{py}	0.025 m
Piezoceramic thickness, h_p	2.50×10^{-4} m
Piezoceramic Young's Modulus, E_p	6.70×10^{10} N/m^2
Charge constant, d_{31}	-2.10×10^{-10} m/V
Voltage constant, g_{31}	-1.15×10^{-2} Vm/N
Capacitance, C	1.05×10^{-7} F
Electromechanical coupling factor, k_{31}	0.34

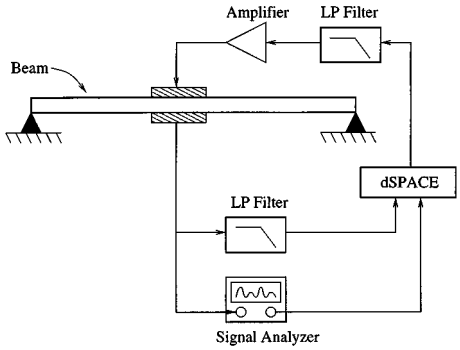

Fig. 4. Experimental setup.

There is still a difficulty in using feedthrough terms in the performance output, $z(x,t)$ (23) since the spatial $\mathcal{H}_2$ norm of the system will not remain finite. To avoid this problem, feedthrough terms are replaced with second-order out-of-bandwidth terms as suggested in [1]. It has to be ensured that the second-order term has a zero-frequency content that is close to (23). The resonant frequency of the second-order system, ω_c, is set above the bandwidth of interest. Also, a relatively high damping ratio, ζ_c, is used, so that the second-order system behaves like a low-pass filter.

Thus the modified system is

$$\begin{aligned} \dot{\tilde{x}}(t) &= \tilde{A}\tilde{x}(t) + \tilde{B}_1 w(t) + \tilde{B}_2 u(t) \\ z(x,t) &= \tilde{C}_1(x)\tilde{x}(t) \\ V_s(t) &= \tilde{C}_2\tilde{x}(t) + D_{21}w(t) + D_{22}u(t) \end{aligned} \tag{24}$$

where $\tilde{x}$ consists of the plant's original states, $\bar{x}$ and the states due to the extra second-order term.

Then, the spatial $\mathcal{H}_2$ control problem is to design a controller

$$\begin{aligned} \dot{x}_k(t) &= A_k x_k(t) + B_k V_s(t) \\ u(t) &= C_k x_k(t) + D_k V_s(t) \end{aligned} \tag{25}$$

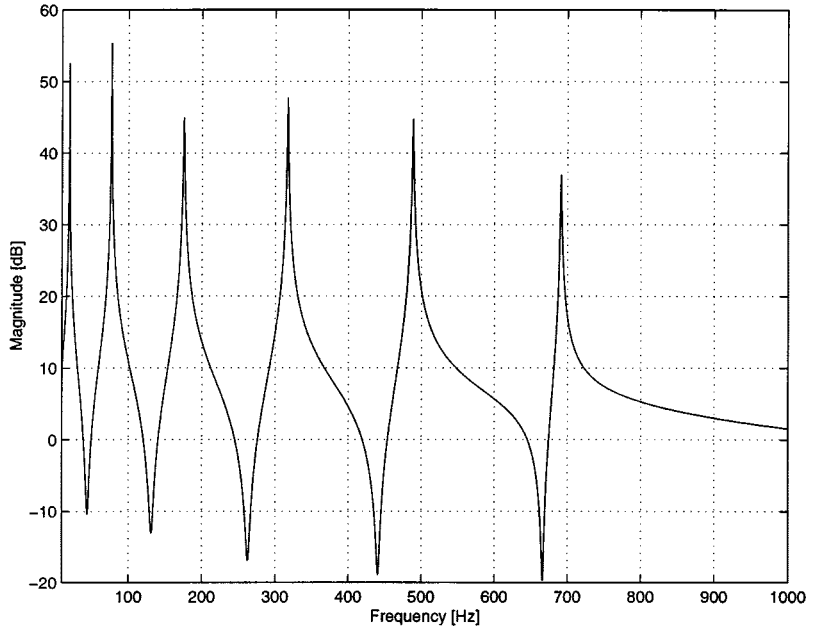

(a)

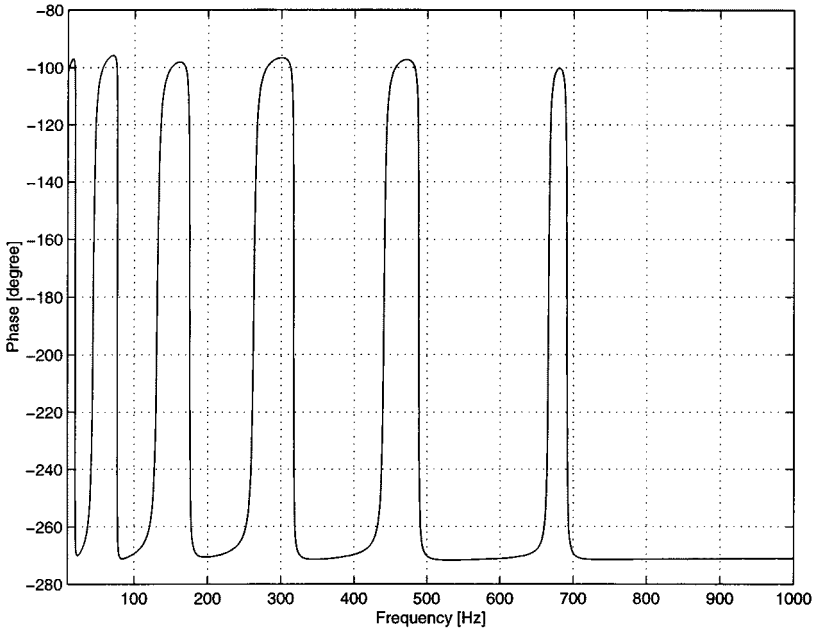

(b)

Fig. 5. Frequency response of the controller (input voltage to output voltage [V/V]).

such that the closed-loop system minimizes the weighted spatial $\mathcal{H}_2$ norm the closed-loop system [6], [16]

$$\ll T_{zw}(s,x) \gg_{2,Q}^2 = \frac{1}{2\pi}\int_{-\infty}^{\infty}\int_X tr\left\{T_{zw}(j\omega,x)^* Q(x) T_{zw}(j\omega,x)\right\} dx d\omega. \quad (26)$$

Here, $Q(x)$ is a spatial weighting function and T_{zw} is the closed-loop transfer function from w to z. The purpose of $Q(x)$ is to emphasize the region where the vibration is to be damped more heavily. In this particular application, $Q(x) = 1$. In other words, the entire beam is weighted equally.

It can be shown, using the method in Section III, that the above problem is equivalent to a standard $\mathcal{H}_2$ control problem for the following system:

$$\begin{aligned}\dot{\tilde{x}}(t) =& \tilde{A}\tilde{x}(t) + \tilde{B}_1 w(t) + \tilde{B}_2 u(t)\\ \tilde{z}(t) =& \Gamma\tilde{x}(t)\\ V_s(t) =& \tilde{C}_2\tilde{x}(t) + D_{21}w(t) + D_{22}u(t)\end{aligned} \quad (27)$$

where $D_{21} = D_{22}$ and Γ is any matrix that satisfies

$$\Gamma^T\Gamma = \int_X \tilde{C}_1(x)^T \tilde{C}_1(x) dx. \quad (28)$$

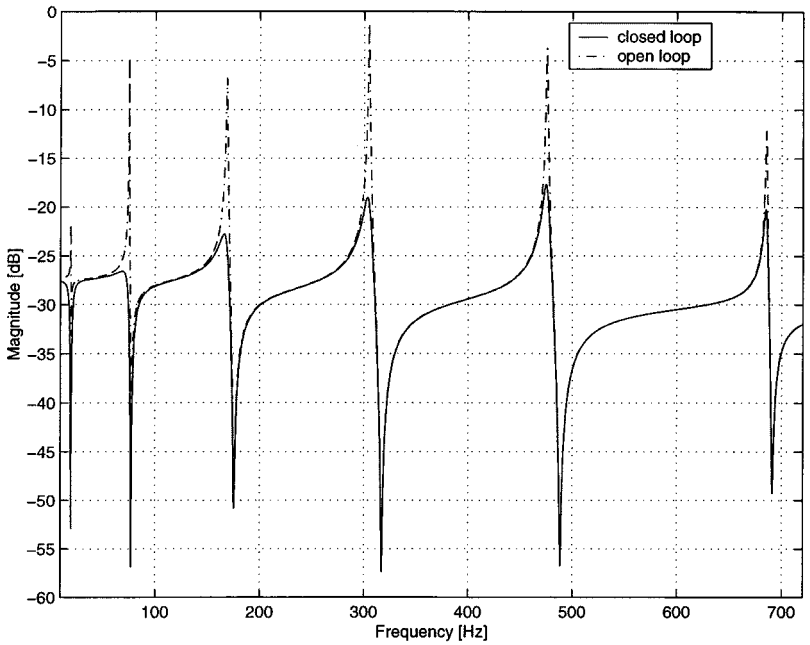

(a)

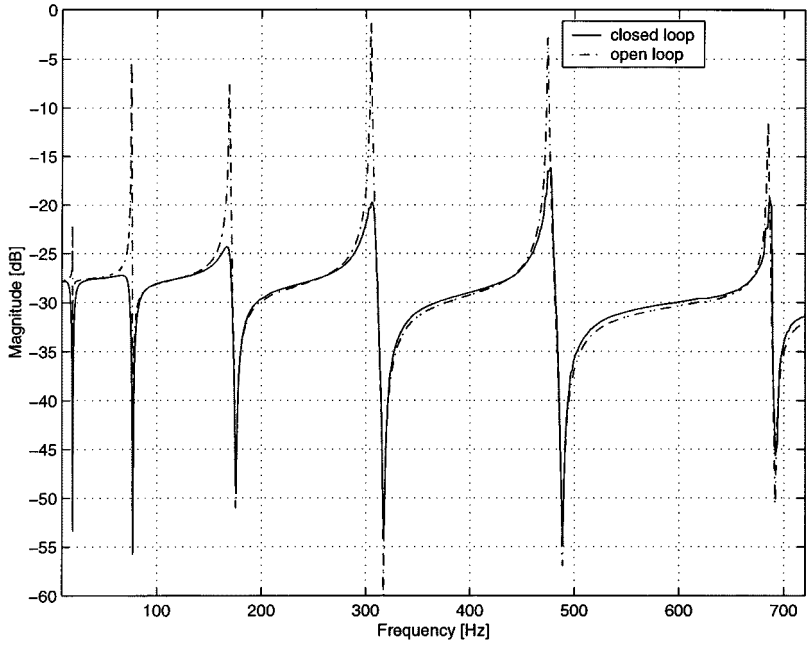

(b)

Fig. 6. Simulation and experimental frequency responses (actuator voltage to sensor voltage [V/V]).

Hence, the system in (27) can be solved using a standard $\mathcal{H}_2$ control technique. The spatial $\mathcal{H}_2$ controller can be regarded as a controller that reduces structural vibration in an average sense.

Designing a $\mathcal{H}_2$ controller for the system (27) may result in a very high gain controller, which may not have the required robustness properties. This problem can be addressed by introducing a weight factor, r, on the control signal. This can be achieved by rewriting (27) as

$$\begin{aligned}\dot{\tilde{x}}(t) =& \tilde{A}\tilde{x}(t) + \tilde{B}_1 w(t) + \tilde{B}_2 u(t)\\ \hat{z}(t) =& \begin{bmatrix}\Gamma\\ 0\end{bmatrix}\tilde{x}(t) + \begin{bmatrix}0\\ r\end{bmatrix}u(t)\\ V_s(t) =& \tilde{C}_2\tilde{x}(t) + D_{21}w(t) + D_{22}u(t).\end{aligned} \tag{29}$$

In practice, one has to make a compromise between the level of vibration reduction and controller gain by choosing a suitable r.

VI. Controller Design

This section explains the details of a spatial $\mathcal{H}_2$ controller that is designed and implemented on a simply supported flexible beam in the Laboratory for Dynamics and Control of Smart Structures at the University of Newcastle, Australia. A simply supported flexible beam with a collocated piezoelectric actuator-sensor pair attached to it is used in the experiments. The apparatus is mounted on an optical table and is shown in Fig. 3. The structure consists of a 60 cm long uniform aluminum beam

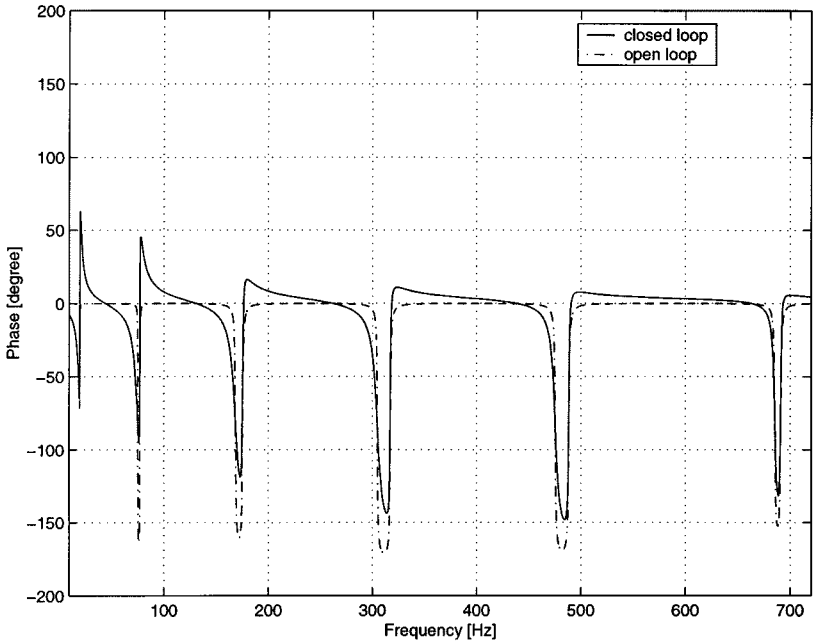

(c)

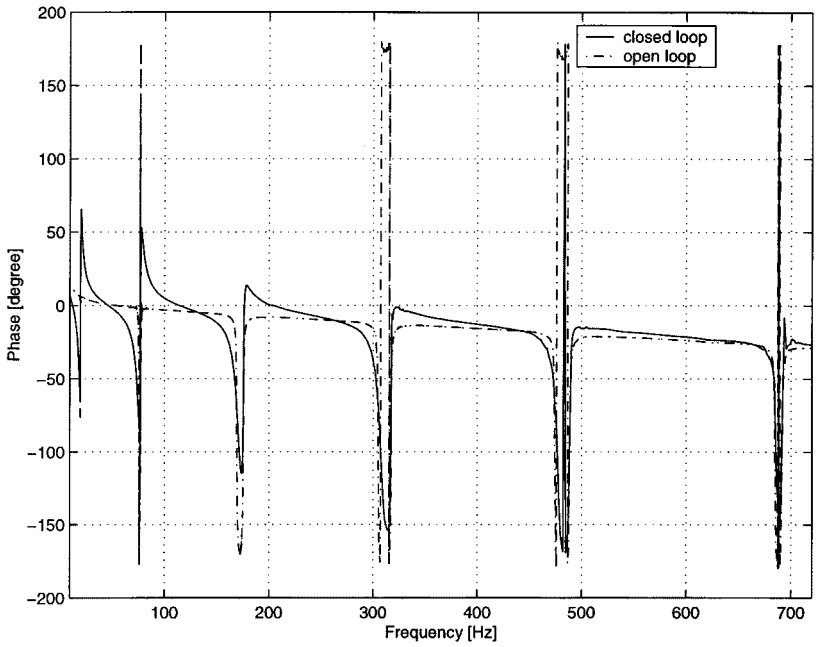

(d)

Fig. 6. (*Continued*.) Simulation and experimental frequency responses (actuator voltage to sensor voltage [V/V]).

of a rectangular cross section (50 mm $\times$ 3 mm). The beam is pinned at both ends. A pair of piezoelectric ceramic elements is attached symmetrically to either side of the beam, 50 mm away from one end of the beam. The piezoceramic elements used in the experiment are PIC151 patches. These patches are 5 mm wide, 70 mm long, and 0.25 mm thick. The physical parameters of PIC151 are given in Table I. A model of the piezoelectric laminate beam is obtained via modal analysis (see the Appendix). The equivalent standard $\mathcal{H}_2$ control problem described in (29) is used for the proposed spatial $\mathcal{H}_2$ controller. Here, V_s is the output voltage from the piezoelectric sensor, while u is the control input voltage applied to the actuating patch.

In this paper, a SISO controller is designed for the purpose of controlling only the first six vibration modes of the beam. Hence, the model is truncated to include only the first six bending modes. The effect of out-of-bandwidth modes has to be taken into consideration to correct the locations of the in-bandwidth zeros of the truncated model as discussed in Section IV. Based on the experimental frequency-response data from actuator voltage to sensor voltage and using a

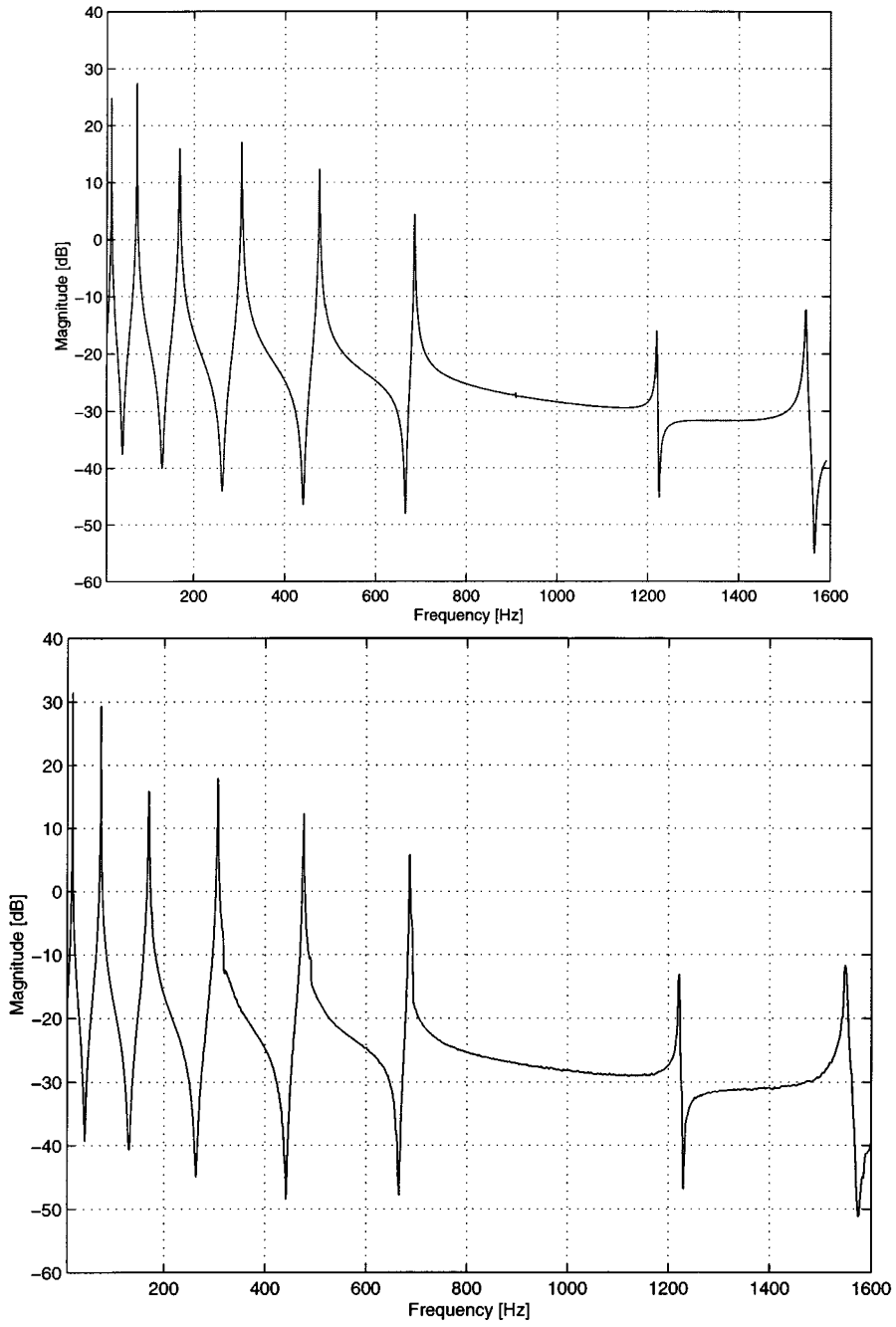

Fig. 7. Loop gain [V/V]: simulation and experiment.

technique similar to [17], the feedthrough term in (16), $D_{21} = D_{22} = K_{Vs}$, is found to be 0.033 if the first six modes are considered in the model.

Since the disturbance is assumed to enter the system through the same channel as the controller, the SISO transfer functions from w and u to the transverse deflection of the beam, $z(x,t)$, are the same, i.e., $G^N(s,x)$. Considering (21) and (22) in (19)

$$G^N(s,x) = \sum_{k=1}^{N} \frac{W_k(x)\bar{\Psi}_k}{s^2 + 2\zeta_k\omega_k s + \omega_k^2} + \sum_{k=N+1}^{N_{\max}} K_k^{opt} W_k(x) \tag{30}$$

where $\bar{\Psi}_k$ is a scalar since $M = 1$.

Notice that $N = 6$ since it is desirable to find a controller of minimal order to control the first six modes of the structure. The feedthrough term is calculated by considering modes $N+1$ to $N_{\max} = 200$ to obtain a reasonable spatial approximation to the feedthrough term. Similarly, the SISO transfer functions from w and u to the collocated sensor voltage, V_s, are denoted by $G_{V_s}^N(s)$ (16)

$$G_{V_s}^N(s) = \Upsilon \sum_{k=1}^{N} \frac{\bar{\Psi}_k^2}{s^2 + 2\zeta_k\omega_k s + \omega_k^2} + K_{Vs} \tag{31}$$

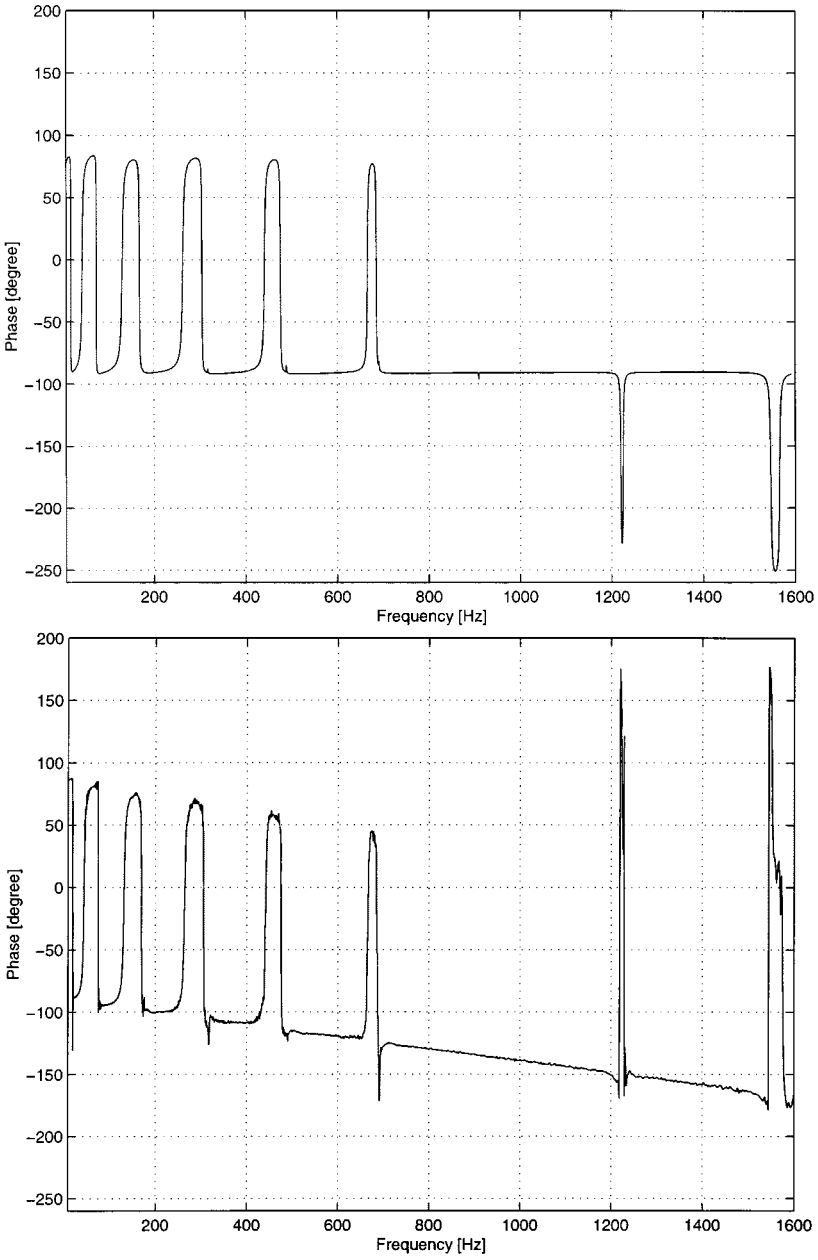

Fig. 7. (*Continued*.) Loop gain [V/V]: simulation and experiment.

The state-space model of the spatial $\mathcal{H}_2$ control problem can be defined as

$$\tilde{A} = \begin{bmatrix} 0_{N+1\times N+1} & I_{N+1\times N+1} \\ \tilde{A}1_{N+1\times N+1} & \tilde{A}2_{N+1\times N+1} \end{bmatrix}$$

where

$$\begin{aligned} \tilde{A}_1 =& -diag\left(\omega_1^2,\ldots,\omega_N^2\omega_c^2\right) \\ \tilde{A}_2 =& -2diag\left(\zeta_1\omega_1,\ldots,\zeta_N\omega_N,\zeta_c\omega_c\right) \end{aligned}$$

and

$$\begin{aligned} \tilde{B}_1 =& \tilde{B}_2 = [0,\ldots,0,0,\Psi_{11},\ldots,\Psi_{N1},1]^T \\ \tilde{C}_1(x) =& \Big[W_1(x),\ldots,W_N(x) \\ & \omega_c^2 \sum_{k=N+1}^{N_{\max}} K_k^{opt} W_k(x),0,\ldots,0,0\Big] \\ \tilde{C}_2 =& \Upsilon\left[\Psi_{11},\ldots,\Psi_{N1},0,0,\ldots,0,0\right] \\ D_{21} =& D_{22} = K_{Vs}. \end{aligned} \tag{32}$$

Based on (28), Γ can be obtained for the performance output $\hat{z}$ in (29) using the orthogonality property in (3)

$$\Gamma = \begin{bmatrix} \tilde{\Gamma}_{N+1\times N+1} & 0_{N+1\times N+1} \\ 0_{N+1\times N+1} & 0_{N+1\times N+1} \end{bmatrix} \tag{33}$$

where $\tilde{\Gamma} = \text{diag}\left(1,\ldots,1,\omega_c^2\left(\sum_{k=N+1}^{N_{\max}}\left(K_k^{opt}\right)^2\right)^{1/2}\right)$.

Matlab μ-Analysis and Synthesis Toolbox was used to design the spatial $\mathcal{H}_2$ controller based on the system in (29) via a state-space approach.

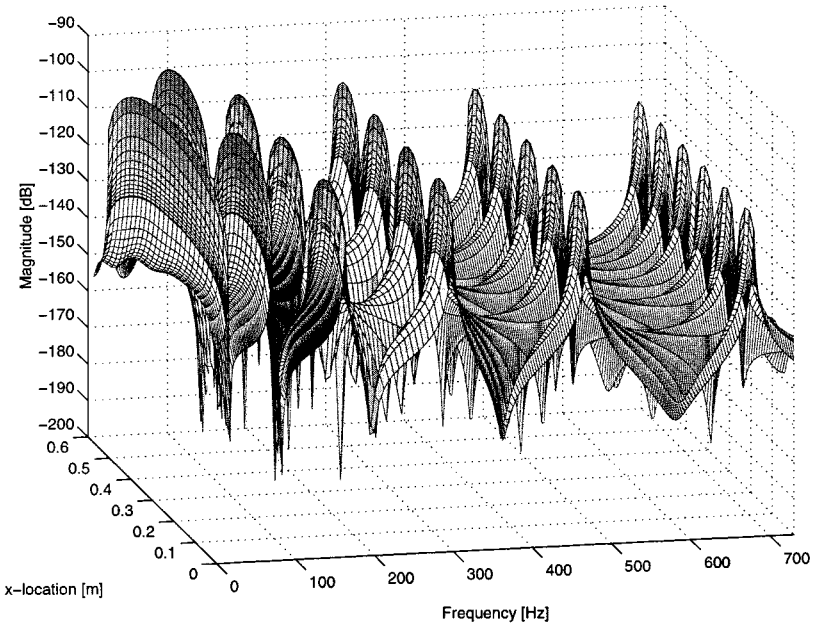

Fig. 8. Simulated spatial frequency response: open-loop actuator voltage to beam deflection [m/V].

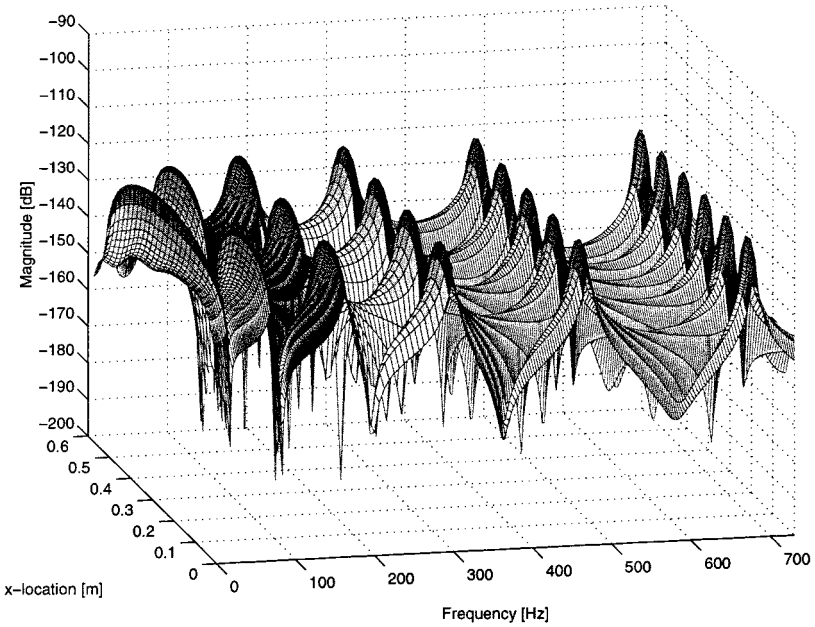

Fig. 9. Simulated spatial frequency response: closed-loop actuator voltage to beam deflection [m/V].

VII. Experimental Implementation

The experimental setup is depicted in Fig. 4. The controller was implemented using a dSpace DS1103 rapid prototyping Controller Board together with the Matlab and Simulink software. The sampling frequency was set at 20 KHz, while the cutoff frequencies of the two low-pass filters were set at 3 KHz. A high-voltage amplifier, capable of driving highly capacitive loads, was used to supply necessary voltage for the actuating piezoelectric patch. An HP89410A Dynamic Signal Analyzer and a Polytec PSV-300 Laser Doppler Scanning Vibrometer were used to obtain frequency responses of the piezoelectric laminate beam. Important parameters of the beam, such as resonant frequencies and damping ratios, were obtained from the experiment and were used to correct the model.

The frequency response of the controller is shown in Fig. 5. The controller has a resonant nature because of the highly resonant nature of the beam, i.e., the controller attempts to apply a high gain at each resonant frequency to minimize the resonant response. Fig. 6 compares frequency responses of the open-loop and closed-loop systems (actuator voltage to sensor voltage) for both simulation and experimental results. The performance of the controller applied to the real system is as expected from the simulation. The resonant responses of the first six modes have been reduced considerably once the controller was introduced.

Fig. 7 compares the loop gain up to 1.6 KHz from simulation and experiment. The simulation gives a gain margin of 12.4 dB at 1.55 KHz and a phase margin of 88.4° at 78.5 Hz. The experiment gives a gain margin of 15.7 dB at 1.22 KHz and a phase margin of 87.0° at 79.1 Hz.

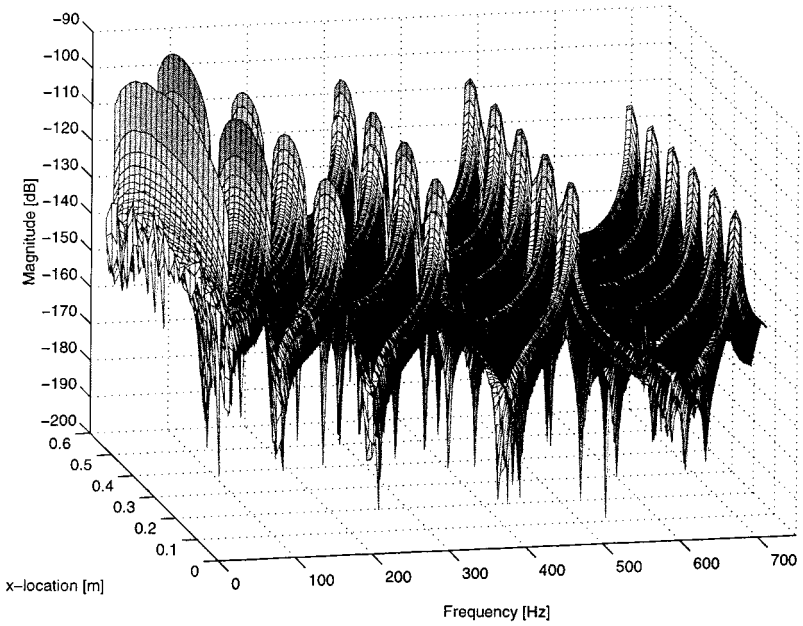

Fig. 10. Experimental spatial frequency response: open-loop actuator voltage to beam deflection [m/V].

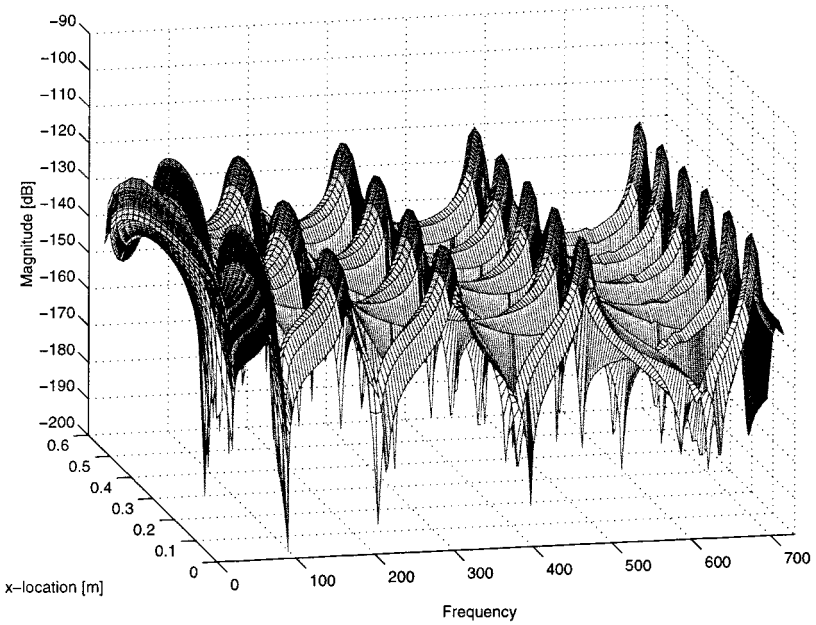

Fig. 11. Experimental spatial frequency response: closed-loop actuator voltage to beam deflection [m/V].

Figs. 8 and 9 show the simulated spatial frequency responses of the uncontrolled and controlled beam, respectively. Here, x is measured from one end of the beam, which is closer to the patches. The spatial frequency responses were also obtained from the experiments. A Polytec PSV-300 Laser Scanning Vibrometer was used to obtain the frequency response of the beam's vibration at a number of points on the surface. The spatial frequency responses of the uncontrolled and controlled beam are shown in Figs. 10 and 11. It is observed that the resonant responses of the first six modes have been reduced over the entire beam due to the controller action, which is as expected from the simulation (compare with Figs. 8 and 9). The resonant responses of modes 1–6 have been reduced by approximately 25.5, 28.5, 18, 18, 14 and 7 dB, respectively, over the entire beam. Notice that the amount of vibration reduction is greater for low-frequency modes than for high-frequency modes. This is expected since low-frequency modes generally contribute more to the spatial $\mathcal{H}_2$ norm of the system as can be seen in (8) and (9). This is beneficial since low-frequency modes are often the significant contributors to vibrations of flexible structures.

To show the advantage of the spatial $\mathcal{H}_2$ control over the pointwise $\mathcal{H}_2$ control, the following simulation was performed. Based on the designed spatial $\mathcal{H}_2$ controller, $\mathcal{H}_2$ norm of the controlled and uncontrolled beam has been plotted as a function of x in Fig. 12(a). Next, a pointwise $\mathcal{H}_2$ controller was designed to minimize the deflection at the middle of the beam,

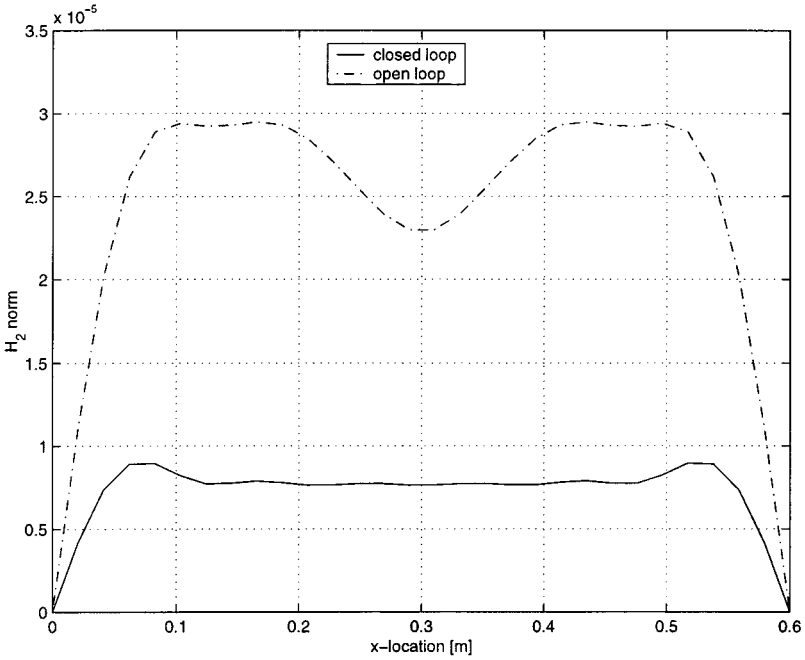

(a)

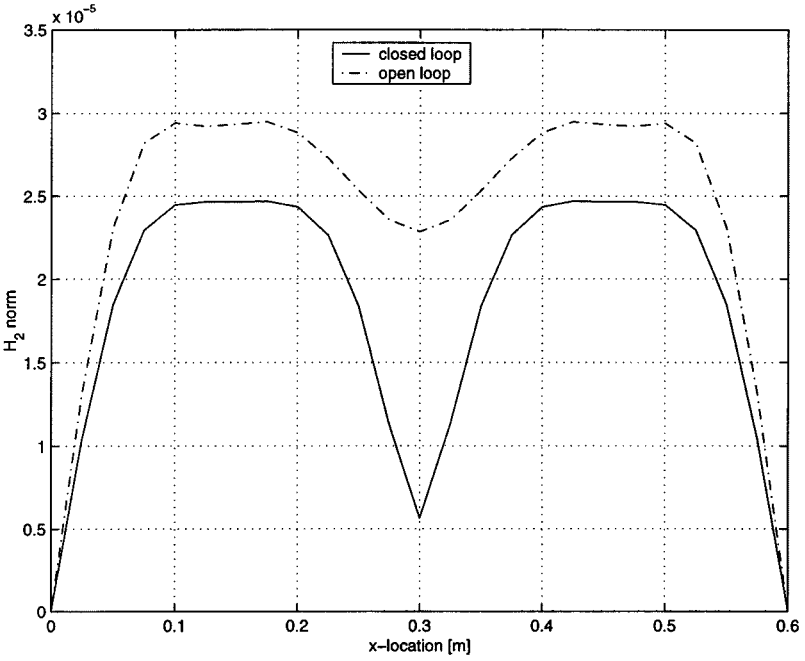

(b)

Fig. 12. Simulated $\mathcal{H}_2$ norm plots.

i.e., $x = 0.3$ m. The controller had a gain margin of 12.7 dB and a phase margin of 87.6°. Based on this pointwise controller, $\mathcal{H}_2$ norm of the controlled and uncontrolled beam has also been plotted as a function of x in Fig. 12(b).

Fig. 12(a) clearly demonstrates the effect of the proposed spatial $\mathcal{H}_2$ controller in reducing the vibration of the beam. It is obvious that the $\mathcal{H}_2$ norm of the entire beam has been reduced by the action of the controller in a more uniform manner. The highest $\mathcal{H}_2$ norm of the uncontrolled beam has been reduced by approximately 69.5%, from 2.95×10^{-5} to 9.0×10^{-6}.

Meanwhile, Fig. 12(b) shows the effectiveness of the pointwise control in local reduction of the $\mathcal{H}_2$ norm, especially at and around $x = 0.3$ m. This is expected since the purpose of this controller is to minimize vibration at $x = 0.3$ m. In fact, the pointwise controller only suppresses the odd numbered modes since $x = 0.3$ m is a node for even numbered modes. Comparing Fig. 12(a) and (b), it can be concluded that the spatial $\mathcal{H}_2$ controller has an advantage over the pointwise $\mathcal{H}_2$ controller as it minimizes the vibration throughout the entire structure.

Fig. 13 shows the controller's effectiveness in minimizing beam's vibration in time domain. A step disturbance signal was applied through the piezoelectric actuator. The velocity response at the middle of the beam was observed using the PSV Laser Vibrometer. The velocity response was filtered by a

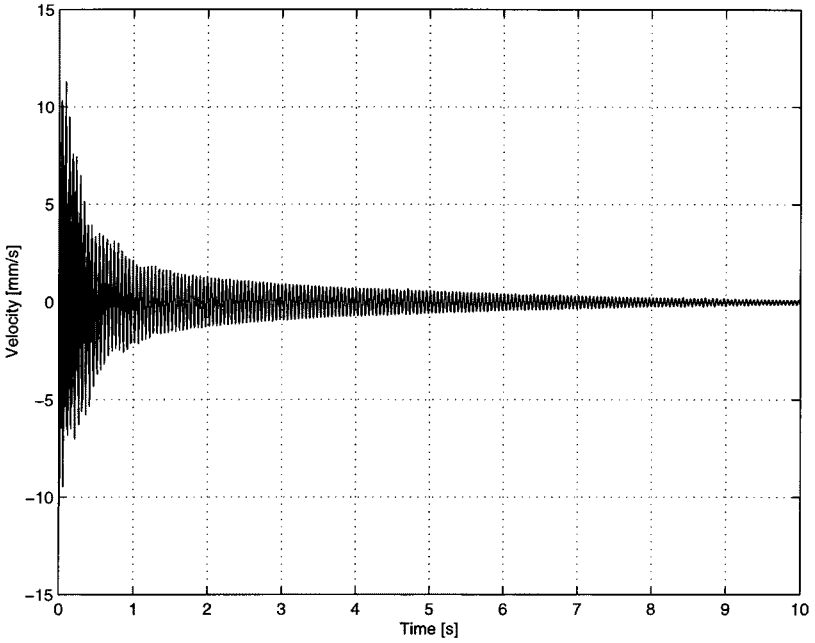

(a)

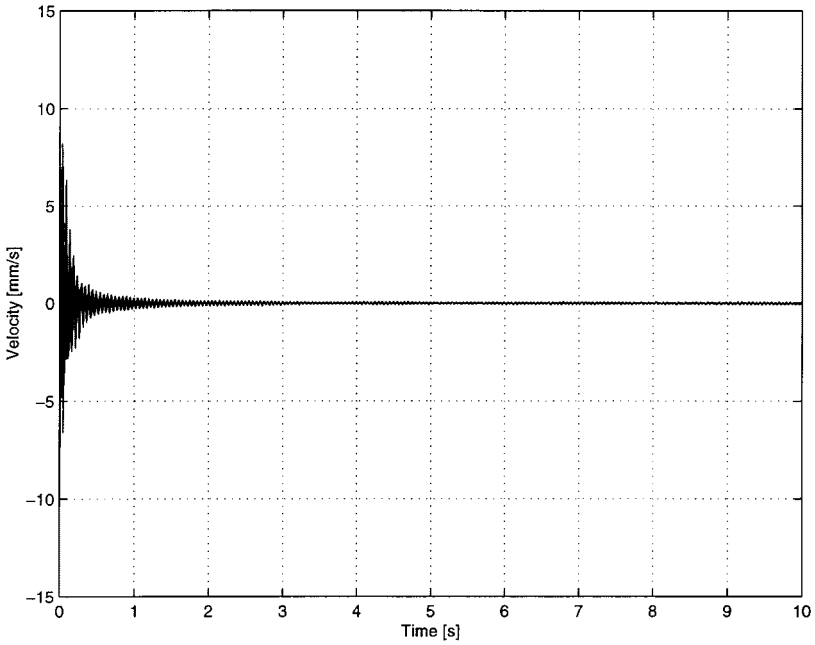

(b)

Fig. 13. Vibration at the middle of the beam.

low-pass filter with a cutoff frequency of 750 Hz. It can be seen that the settling time of the velocity response has been reduced considerably because of the controller's action.

VIII. Conclusion

A spatial $\mathcal{H}_2$ controller was designed and implemented on a piezoelectric laminate beam. It was observed that such a controller resulted in suppression of transverse vibrations of the entire structure by minimizing the spatial $\mathcal{H}_2$ norm of the closed-loop system. The controller was obtained by solving a standard $\mathcal{H}_2$ control problem for a finite-dimensional system. Feedthrough terms were added to correct the locations of in-bandwidth zeros of the system. The experiments showed the effectiveness of the controller in reducing the structural vibrations on a piezoelectric laminate beam. It was shown that the spatial $\mathcal{H}_2$ control has an advantage over the pointwise $\mathcal{H}_2$ control in minimizing structural vibration of the entire structure. The spatial $\mathcal{H}_2$ control minimizes the $\mathcal{H}_2$ norm of the entire structure more uniformly, while the pointwise $\mathcal{H}_2$ control minimizes the $\mathcal{H}_2$ norm more locally. The application of this spatial $\mathcal{H}_2$ control is not confined to a piezoelectric laminate beam. It may be applied to more general vibration suppression problems.

APPENDIX
MODAL SOLUTION OF A SIMPLY-SUPPORTED BEAM

Consider a flexible beam with simply-supported or pinned ends. A simply supported beam has the following boundary conditions:

$$z(L,t) = z(0,t) = 0 \tag{34}$$

$$\frac{\partial^2 z(0,t)}{\partial x^2} = \frac{\partial^2 z(L,t)}{\partial x^2} = 0. \tag{35}$$

The first boundary condition signifies that the transverse deflections at the beam's ends are restricted. The last equation signifies zero moment at the beam's ends since there is no rotational restriction at the ends. The transverse deflection is $z(x,t) = \sum_{k=1}^{\infty} W_k(x) q_k(t)$. The eigenfunction that satisfies the boundary conditions and the eigenvalue problem can be shown to be a sinusoidal function:

$$W_k(x) = \sqrt{\frac{2}{L}} \sin\left(\frac{k\pi x}{L}\right). \tag{36}$$

The orthogonality properties of the eigenvectors are as in (3) and (4), where the natural frequency at any mode k obtained from the solution of the eigenvalue problem is

$$\omega_k = \left(\frac{k\pi}{L}\right)^2 \sqrt{\frac{EI}{\rho A_b}}. \tag{37}$$

REFERENCES

[1] R. L. Clark, "Accounting for out-of-bandwidth modes in the assumed modes approach: Implications on colocated output feedback control," *Trans. ASME*, vol. 119, pp. 390–395, September 1997.

[2] S. O. R. Moheimani, "Minimizing the effect of out-of-bandwidth dynamics in the models of reverberant systems that arise in modal analysis: Implications on spatial $\mathcal{H}_\infty$ control," *Automatica*, vol. 36, pp. 1023–1031, 2000.

[3] ——, "Minimizing the effect of out of bandwidth modes in truncated structure models," *ASME J. Dyn. Syst., Measurement, Contr.*, vol. 122, pp. 237–239, March 2000.

[4] S. O. R. Moheimani and W. P. Heath, "Model correction for a class of spatio-temporal systems," *Automatica*, vol. 38, no. 1, pp. 147–155, 2002.

[5] R. L. Bisplinghoff and H. Ashley, *Principles of Aeroelasticity*. New York: Dover, 1975.

[6] S. O. R. Moheimani and T. Ryall, "Considerations in placement of piezoceramic actuators that are used in structural vibration control," in *Proc. 38th IEEE Conf. Decision Contr.*, Phoenix, AZ, December 1999, pp. 1118–1123.

[7] R. L. Clark, W. R. Saunders, and G. P. Gibbs, *Adaptive Structures: Dynamics and Control*. New York: Wiley, 1998.

[8] E. K. Dimitriadis, C. R. Fuller, and C. A. Rogers, "Piezoelectric actuators for distributed vibration excitation of thin plates," *ASME J. Vibration Acoust.*, vol. 113, pp. 100–107, Jan. 1991.

[9] C. R. Fuller, S. J. Elliot, and P. A. Nelson, *Active Control of Vibration*. New York: Academic, 1996.

[10] H. T. Banks, R. C. Smith, and Y. Wang, *Smart Material Structures: Modeling, Estimation and Control*. Chichester, U.K.: Wiley-Masson, 1996.

[11] H. R. Pota and T. E. Alberts, "Multivariable transfer functions for a slewing piezoelectric laminate beam," *ASME J. Dyn. Syst., Measurement, Contr.*, vol. 117, pp. 352–359, Sept. 1995.

[12] I. R. Petersen and H. R. Pota, "Minimax LQG optimal control of a flexible beam," in Proc. 3rd IFAC Symp. Robust Contr. Design, Prague, 2000.

[13] L. Meirovitch, *Elements of Vibration Analysis*. New York: McGraw Hill, 1975.

[14] T. E. Alberts and J. A. Colvin, "Observations on the nature of transfer functions for control of piezoelectric laminates," *J. Intell. Material Syst. Structures*, vol. 8, no. 5, pp. 605–611, 1991.

[15] T. E. Alberts, T. V. DuBois, and H. R. Pota, "Experimental verification of transfer functions for a slewing piezoelectric laminate beam," *Contr. Eng. Practice*, vol. 3, no. 2, pp. 163–170, 1995.

[16] S. O. R. Moheimani and M. Fu, "Spatial $\mathcal{H}_2$ norm of flexible structures and its application in model order selection," in *Proc. 37th IEEE Conf. Decision Contr.*, Tampa, FL, Dec. 1998, pp. 3623–3624.

[17] S. O. R. Moheimani, "Experimental verification of the corrected transfer function of a piezoelectric laminate beam," *IEEE Trans. Contr. Syst. Technol.*, vol. 8, no. 4, pp. 660–666, July 2000.

Dunant Halim (S'00) was born in Jakarta, Indonesia, in 1974. He received the B.Eng. degree with first class honors in aerospace engineering from the Royal Melbourne Institute of Technology, Australia, in 1999. He is currently pursuing the Ph.D. degree in the School of Electrical Engineering and Computer Science at the University of Newcastle, Australia.

His current research is in vibration control of smart structures.

S. O. Reza Moheimani (S'93–M'97–SM'00) was born in Shiraz, Iran, in 1967. He received the B.Sc. degree from Shiraz University, Shiraz, Iran, in 1990 and the M.Eng.Sc. and Ph.D. degrees from the University of New South Wales, Australia, in 1993 and 1996, all in electrical and electronics engineering.

In 1996, he was a Postdoctoral Research Fellow at the School of Electrical and Electronics Engineering, Australian Defence Force Academy, Canberra. In 1997, he joined the University of Newcastle, where he is currently a Senior Lecturer in the School of Electrical Engineering and Computer Science. He is a member of the Centre for Integrated Dynamics and Control, an Australian Government Special Research Centre. He is interested in smart structures, mechatronics, control theory, and signal processing. He is an Associate Editor for *Control Engineering Practice*.

Dr. Moheimani is a Member of IFAC Technical Committee on Mechatronic Systems. He is currently serving on editorial boards of several international conferences, including the Second IFAC Conference on Mechatronic Systems, to be held in Berkeley, CA, in December 2002.